

MRI TRACER STUDY OF THE CEREBROSPINAL FLUID DRAINAGE PATHWAY IN NORMAL AND HYDROCEPHALIC GUINEA PIG BRAIN

Shinya YAMADA*¹, Masayoshi SHIBATA*², Merium SCADENG*⁵, Stefan BLUML*⁴, Catherine NGUY*⁶, Brian ROSS*⁶ and J. Gordon McCOMB*³

**¹Department of Neurosurgery, Tokai University Oiso Hospital*

**²Department of Neurosurgery, Tokai University Hospital*

*Divisions of *³Neurosurgery and *⁴Radiology, Children's Hospital Los Angeles and The Keck School of Medicine, University of Southern California*

**⁵Rudi Schulte Research Institute, Santa Barbara*

**⁶Huntington Medical Research Institute, Pasadena*

(Received October 26, 2004; Accepted December 16, 2004)

OBJECTIVE: Using magnetic resonance imaging (MRI), sequential information regarding the dynamic movement of the cerebrospinal fluid (CSF) from the subarachnoid space and the ventricles to the drainage pathway in response to the CSF pressure was obtained in guinea pigs. In this study, a new mechanical hydrocephalus model in a guinea pig was developed to investigate the CSF kinetics in an acute hydrocephalic brain.

MATERIALS AND METHODS: A total of 18 adult male guinea pigs were studied. In the ventricular injection group, The CSF in the lateral and third ventricles was isolated by inserting a polyethylene tube with a cotton ball into the aqueduct of Sylvius. By infusing artificial CSF through this tubing acute ventriculomegaly was created. In the subarachnoid injection group, a polyethylene tube was placed at the cisterna magna. Using MRI with gadoteridol as a tracer, the movement of CSF from the subarachnoid space and dilated ventricles was monitored at various pressures. The CSF drainage pathway from the subarachnoid space in the hydrocephalic condition was examined and compared with the CSF drainage pathway in normal condition.

RESULTS: Gadoteridol cleared from the lateral and third ventricles and reached the nasal mucosa via brain parenchyma; the movement was proportional to the CSF pressure. Gadoteridol from the subarachnoid space also reached the nasal mucosa and periorbital region in a similar manner. However, it was not observed to reach either over the convexity of the brain or adjacent to the superior sagittal sinus.

Key words : Cerebrospinal fluid drainage pathway, Hydrocephalus, Magnetic resonance imaging

INTRODUCTION

Under normal physiological conditions, most of the cerebrospinal fluid (CSF) is secreted by the choroid plexus and flows through the ventricular system to emerge from the fourth ventricle. The CSF then traverses the subarachnoid spaces via unidirectional open channels due to the difference in hydrostatic pressure. It has been widely believed that the arachnoid granules (or arach-

noid villi) are the main drainage site of the CSF. This pathway is known as the classical pathway of CSF drainage [1, 2]. On the other hand, several investigations have revealed that a considerable fraction of the CSF and brain interstitial fluid drains into the non-arachnoidal-granulation pathway [3-12] Until recently, this pathway was referred to as an alternative, substantial, or lesser pathway of CSF drainage, implying that this pathway is insignificant. However, some investigators

showed that more than 14% to 47% clearance of the tracers administered into the CSF were cleared via this pathway [3, 6, 10, 13]. In the alternative pathway, the CSF or brain interstitial fluids drains into the nasal mucosa or periorbital region through an open channel around the nerve sheath and subsequently into the deep cervical lymphatic system [3, 4, 6-8, 11, 14, 15]. However, these studies were limited to either morphological or radioisotope studies that provided evidence of these drainage pathways as individual data points after injection of tracers into the CSF. These methods used tracers as CSF markers in individuals at a single time point. In this study, MRI was used to obtain sequential information regarding the CSF drainage pathway. It has been identified that CSF kinetics is altered in the presence of a hydrocephalus [1, 12, 16-18]. No suitable animal model has been available for investigation of the pathophysiological changes in the CSF drainage in a hydrocephalic brain. Kaolin-induced hydrocephalus is the most widely used hydrocephalus model for experiments in small animals [19]. Kaolin injected into the subarachnoid space results in inflammatory changes in the arachnoid membrane and brain; subsequently, adhesions are formed to block the CSF pathway. Later, hydrocephalus develops due to an increase in the resistance to CSF outflow [19]. However, in this model, the CSF outflow pressure and the site of blockage is unpredictable, making it unfeasible to study CSF drainage in a hydrocephalic brain. Therefore, the author developed a new hydrocephalus model to monitor the CSF outflow from the lateral ventricle in a hydrocephalic brain. In this new model, hydrocephalus was developed in response to the CSF pressure without inducing inflammation. In addition, this model allows control over the CSF pressure in the lateral ventricle in order to monitor alterations in the amount of CSF drainage and pathway. This study in guinea pigs was conducted in order to obtain sequential information regarding the dynamic movement of CSF from the subarachnoid space and the ventricular system into the drainage pathway in response to CSF pressure.

MATERIALS AND METHODS

In this study, a total of 18 adult male guinea pigs, weighing 600-800 g, were used.

All animal studies were done according to the NIH guidelines and approved by the institutional animal care committee. The animals were initially anesthetized with a s.c. injection of 5 mg/kg xylazine combined with 40 mg/kg ketamine (supplemented as necessary). Fifteen milliliters of half tonic saline was injected subcutaneously for maintenance of body fluid volume. The head was shaved and secured in a stereotaxic frame. A heating pad maintained the guinea pig's body temperature at $38.0 \pm 0.5^\circ\text{C}$ during the surgical procedure. The CSF drainage pathway from the subarachnoid space was investigated in the subarachnoid injection group. The model of the ventricle injection group, which mimics the acute obstructive hydrocephalus in a clinical setting, was designed to investigate the movement of the CSF solely from within the ventricle isolated from the CSF in the subarachnoid space. The movement of the CSF in response to CSF pressure was also examined in each group.

Subarachnoid injection group (SAS group)

This group comprised nine guinea pigs. A 1.5-cm sagittal midline incision was made across the calvarium, extending from the bregma to the third cervical spine, and the craniocervical junction was sufficiently exposed to insert a polyethylene tube (PE-10) into the subarachnoid space. After inserting the tube, it was secured by suturing the surrounding dura mater using 8-0 monofilament thread in order to prevent CSF leakage around the tubing system. The skin was sutured using 4-0 nylon thread.

Ventricle injection group (V group)

This group comprised nine guinea pigs. The skin was incised in a manner similar to that in the "SAS group." The suboccipital bone was carefully removed. The dura covering the cerebellum was then incised in the midline to expose the foramen of Magendie. The outlet of the aqueduct of Sylvius was exposed by superior traction of the cerebellum. A PE-10 tube with a cotton ball secured 5 mm proximal to the tip was passed through the aqueduct of Sylvius until the cotton ball was well positioned within the opening of the fourth ventricle. The combination of the tube and cotton ball prevented the circulation of CSF from the third ventricle into the fourth ventricle (Fig. 1). The skin was then

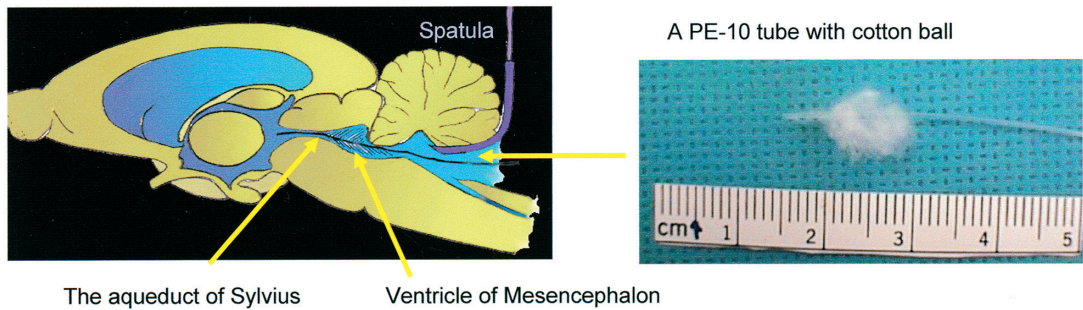


Fig. 1 Left: An illustration of the surgical procedure for the V group. Right: A picture of the insertion catheter for V group.

sutured with 4-0 nylon thread. The isolated CSF drainage route from the lateral ventricle could be examined in this group because the CSF drainage pathway was completely blocked at the aqueduct of Sylvius, and the marker could be directly administered into the ventricle system. This group mimicked the acute obstructive hydrocephalus in a clinical setting and was used to investigate alterations of the CSF drainage route in comparison with the normal physiological CSF drainage route (SAS group).

Infusion of artificial CSF with gadoteridol and indigo carmine into the CSF

Upon completion of the surgical procedure, the animals were placed in a sphinx position inside a specially constructed coil under the MRI scanner. The tubing system that was inserted into either the ventricle or the subarachnoid space was connected to an infusion pump with a long polyethylene tubing (PE-50) system so that the Harvard pump could be placed outside the magnetic field. Fifty microliters of artificial CSF (Elliot's B solution adjusted to a pH of 7.3 by equilibration with CO₂) containing 2 mM gadoteridol (Gd-HP-DO3A) and 0.1% indigo carmine (M.W. 466) was infused through the tubing system at a rate of 20 μ l/min over 5 min into either the subarachnoid space (SAS group) or the intraventricular space (V group). Thereafter, CSF pressure was maintained continuously at various levels (low pressure: 3 cm H₂O, medium pressure: 15 cm H₂O, and high pressure: 40 cm H₂O) by changing the height of the outlet of the infusion system. Three animals were examined in each pressure group both in the V and SAS group. After obtaining a series of MR images over 4 h, cardiac perfusion fixation

was performed at the end of the experiment. The left cardiac ventricle was perfused with 300 ml of isotonic saline containing 3 IU of heparin followed by 900 ml of 10% neutral buffered formalin; the solution was drained out via the right atrium. After the fixation procedure, the skull was removed and localization of the indigo carmine dye in the brain and at the skull base was visually inspected. The animal was maintained under general anesthesia throughout the procedure.

Gadoteridol Concentration Studies

Gadolinium chelate is the most commonly used contrast agent for clinical MRI studies; however, it has been used to a limited extent in the CSF. Since gadolinium compound does not cross the blood brain barrier or the cell membrane, it can be used as an extracellular marker [16, 20]. It has been shown that the ventricular ependymal cell lining is slightly negatively charged. In order to avoid any influence of the tissue charge on the tracer movement, we chose to use gadoteridol, as it has no negative or positive charge (nonionic). Due to the T-2 dominant influence, the signal intensity of high concentration gadoteridol gets converted into hypointensity on T-1 images [21, 22]. Therefore, a gadoteridol concentration study was performed to obtain an appropriate concentration range that would show a semi-quantitative relationship between the concentration of the marker and signal intensity seen on the MR image. However, a controversy exists regarding the method of estimation of actual gadoteridol concentration in the tissue by measuring the intensity of the MR image [21]. Sixteen solutions with graduated dilution from 16 mM to 1.9×10^{-3} mM were scanned using the same parameters that were used for the animal

experiment. An optimal range of gadoteridol was found to be between 2 mM/l to 0.07 mM/l using the T1-sequence along with the coil. Given this range of gadoteridol concentration, signal intensity was observed to convert into hyperintensity on the image immediately after gadoteridol was administered into the CSF.

MR imaging

Magnetic resonance imaging was performed at 1.5 Tesla on a GE Signa. The animal was placed within a specially constructed Helmholtz-type coil with an external diameter of 10 cm. Multiple T1-weighted images were obtained with gradient echo (3D-SPGR-20) (TE/TR (eff)) = 50/7 ms), FOV 8×6 cm², 1.5 mm thickness/0.0 space). The axial and coronal images of the guinea pig were continuously acquired before and after the injection. The experiments continued for 4 h after start of infusion, and axial and coronal images of the guinea pig

were taken every 30 min. The signal intensity in the nasal mucosa, periorbital region, olfactory lobe, and parasagittal region in the images were measured using image analysis software (GE scanner software and NMR win). In order to normalize these data points between each image, a reference point was chosen at the temporalis muscle. The change in signal intensity in the different regions of the CSF drainage pathway against time was plotted. Intensity changes in the region of the individual time points after injection were compared with the values in the same region of pre-infusion image.

RESULTS

Imaging study

The gadoteridol enhancement appeared in the images immediately after it was administered into the CSF in both the SAS and V groups under the T1-sequence. In the V group, coronal views of serial imaging in the guinea pig revealed that gadoteridol

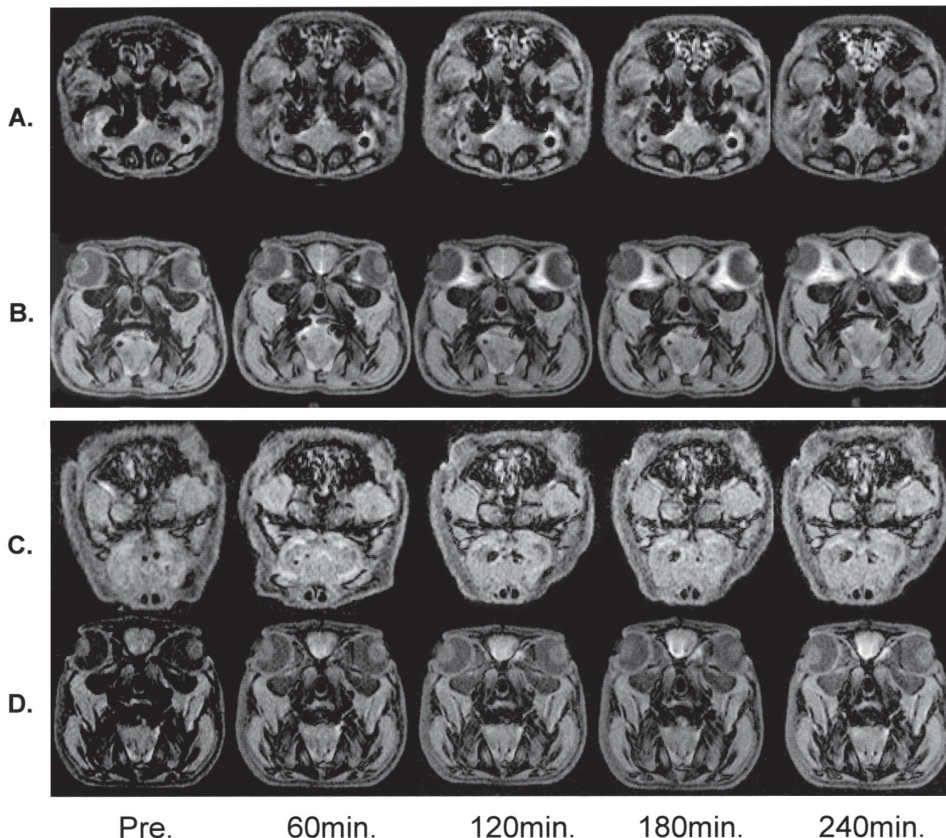


Fig. 2 MR coronal view images. **A:** nasal mucosa (SAS group). **B:** periorbital lesion (SAS group). **C:** nasal mucosa (V group). **D:** olfactory lobes (V group).

enhancement started initially in the olfactory lobes of the brain in the 60-min image followed by the nasal mucosa and periorbital region in the subsequent images. Gadoteridol enhancement in these regions was further increased by the end of the experiment. A similar occurrence was observed in the nasal mucosa and periorbital regions in the SAS group. In the early time period, gadoteridol enhancement observed in the olfactory lobes was less in the SAS group than that in the V group. Little enhancement was observed adjacent to the superior sagittal sinus with almost no evidence of gadoteridol detected over the cerebral convexity over a period of 4 h (Fig. 2). These results indicated that there was no dynamic flow of the CSF in this

region in both groups. A difference between individual animals was observed with regard to the route of CSF drainage. Some animals showed more gadoteridol enhancement in the periorbital region, whereas the others showed more enhancements in the nasal mucosa. It was noted that the drainage pathway to the nasal mucosa and periorbital pathway varied among the individual animals. A relatively large variation was noted within each group; however, not a single animal showed gadoteridol enhancement over the cerebral convexity.

Relation to ICP

The graphs (Fig. 3) show the relationship between signal intensity changes in the dif-

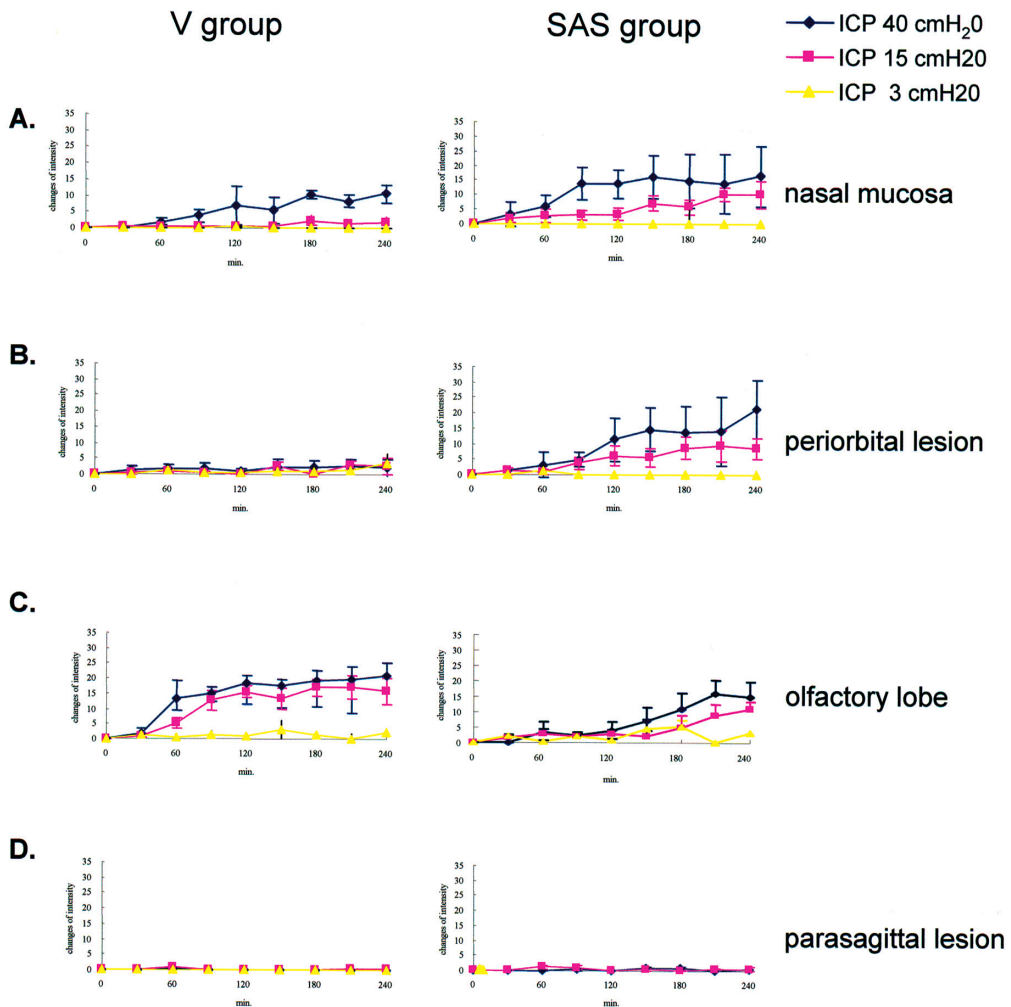


Fig. 3 The graphs show the relationship between signal intensity changes in the different regions of the CSF drainage pathways and in CSF pressure against time in the SAS and V groups. Values were normalized to the signal intensity at the temporalis muscle. **A:** nasal mucosa, **B:** periorbital region, **C:** olfactory lobe, **D:** parasagittal region.

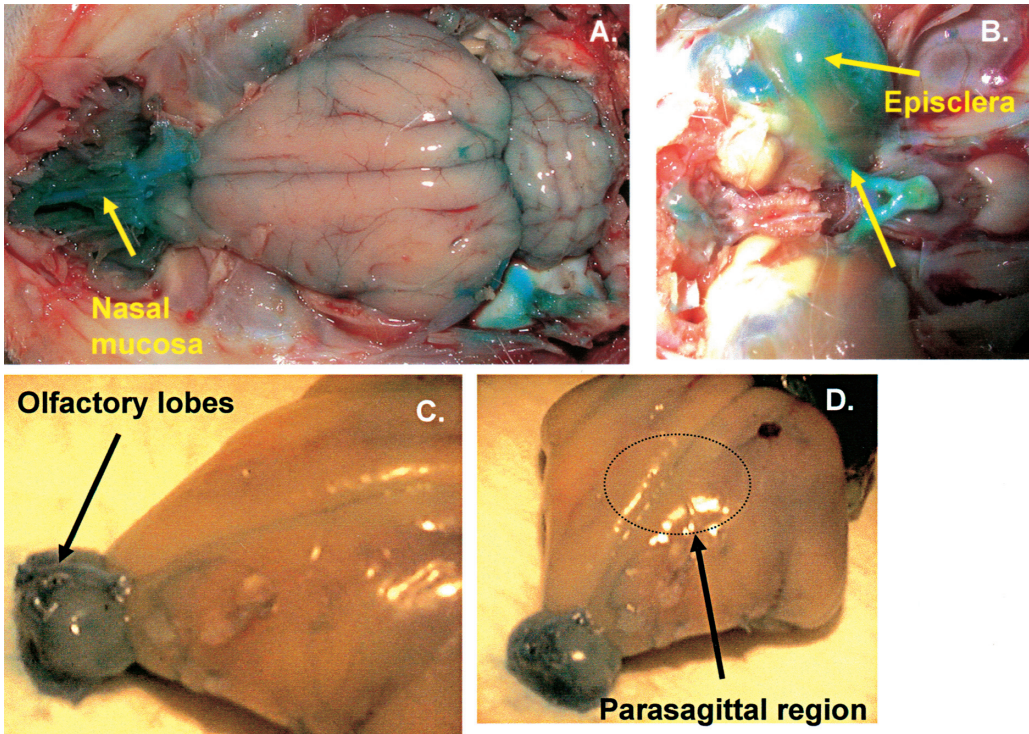


Fig. 4 Visual inspection of dye (indigo carmine) staining of the brain, nasal mucosa, and peri-orbital regions was at the end of experiment (SAS group).
A: nasal mucosa, **B:** periorbital region, **C:** olfactory lobes, **D:** cerebral convexity.

ferent regions of the CSF drainage pathways and in CSF pressure against time in the SAS and V groups. In the high-pressure subgroup of V groups, signal intensity had started to increase in the olfactory lobes and nasal mucosa within 60 min and 90 min, respectively, after the injection. In the medium-pressure subgroup of V group, increase in signal intensity was observed after 90 min in the olfactory lobes. In the low-pressure subgroup of V group, the signal intensity showed negligible increase up to 4 h after start of infusion. In contrast, no early increase in signal intensity was observed in the olfactory lobes in the SAS group prior to the observation in the periorbital region and the nasal mucosa. Thereafter, the signal intensity increased in the olfactory lobe probably due to the exchange of CSF and ISF. Gadoteridol clears faster from central nervous system with greater CSF pressure, implying that the CSF movement is simply a pressure-dependent process. Little intensity change was observed to occur around the superior sagittal sinus region. In addition, gadoteridol was not

detected over the cerebral convexity of the brain in any group over a period of 4 h.

Visual inspection of indigo carmine

Dye (indigo carmine) staining of the brain, nasal mucosa, and periorbital regions was visually inspected at the end of experiment (Fig. 4). The dye was confined to the ventricle system in the V group and to the base of brain in the SAS group. Dye staining was consistently found to some extent in the periorbital region and nasal mucosa even in the low-pressure experimental subgroups. The optic nerve sheath and the episclera were well stained in the periorbital region. Dye staining was found to be more in the periorbital region in some animals, whereas in others it was more in the nasal mucosa. It is again noted that the CSF drainage pathway to the nasal mucosa and periorbital pathway varied for each animal. Dye was found to a lesser extent in the olfactory lobes in the SAS group as compared with that in the V group. No dye was observed over the surface of the brain hemisphere in both groups. These

findings correlated well with the MR images obtained over 4 h.

DISCUSSION

Gadoteridol along with artificial CSF was either infused into the subarachnoid space or directly into the ventricle. The MRI study was conducted in order to obtain sequential information of tracer movement into the nasal mucosa, periorbital region, olfactory lobes, and parasagittal region in response to the CSF pressure alteration. Under T1-sequence, gadoteridol is a very sensitive extracellular tracer. However, a high concentration of gadoteridol appears hypointensity on T1-images due to the significant effect of T2-relaxation time [16, 22]. Gadoteridol appears hyperintensity at an intermediate concentration (2 mM-0.07 mM with T1-sequence). In order to examine the CSF dynamics under MRI in a semi-quantitative manner, it is important to use an appropriate concentration range of gadoteridol in the CSF. Therefore, the actual concentration of gadoteridol in tissues could not be determined from the intensity on the images [16]. The result of this study indicated the presence of CSF drainage pathways to the nasal mucosa and periorbital regions. Drainage of CSF into the nasal mucosa was first described by Schwalbe [15], and this finding has been confirmed on many occasions since then [2, 8, 23]. The CSF pathway to the nasal mucosa is via extension of the subarachnoid space, which surrounds each olfactory filament as it passes through the lamina cribrosa [8]. The pia-arachnoid layers progressively thin and blend into the perineural sheath as the olfactory filament passes through the cribriform plate. This perineural sheath becomes a single cell layer in the nasal mucosa. The perineural spaces between the filament and sheath are reported to be in continuity with the subarachnoid space. The nasal mucosa has numerous lymphatic channels that subsequently drain into the deep cervical lymph nodes. Based on several radioisotope clearance studies on brain, a considerable fraction of the CSF, ranging from 25% to 67%, appears to drain into the lymphatic system, a considerable amount of which takes place via the deep cervical route even under normal physiological CSF pressure in different species of animals, including primates. The periorbital region is another major non-ar-

achnoidal pathway for the CSF clearance [23, 24]. At the termination of the optic nerve subarachnoid space, an area containing numerous small tortuous channels is present with no evidence of the existence of a morphological barrier for movement of macromolecules between the optic nerve subarachnoid space and the periorbital tissue [23]. An MRI makes it possible to visualize real time gadoteridol movement as a bulk flow of CSF that drains into the nasal mucosa and the periorbital region in vivo. A rapid change in signal intensity was observed in the nasal mucosa after the gadoteridol was introduced in both the SAS and V groups. The high-pressure subgroup in the SAS group exhibited greater gadoteridol clearance from the subarachnoid space into the nasal mucosa and periorbital region. An increased change in the intensity was observed in the nasal mucosa and periorbital region following injection of gadoteridol; this was in direct proportion to the CSF pressure in the SAS group. A similar result was observed in the V group as well. More gadoteridol was observed in regions with higher CSF pressure in the V group. In 1914, Weed [25] reported as a microscopic finding that Prussian blue that was injected into the subarachnoid space at the cisterna magna accumulated in the arachnoid granules around the superior sagittal sinus. This site has since been considered a major CSF drainage site and is known as the classical CSF drainage pathway [1, 25]. However, this process required several hours of infusion prior to the appearance of blue granules over the cerebral hemisphere, and, upon visual inspection, no dye was found over convexity of the brain (in the whole series, only one or two small particles were found within the cytoplasm of an endothelial cell in the lining of the superior sagittal sinus). Thus, Weed inferred that the CSF flow in the subarachnoid space over the dorsal surface of the hemisphere is "very sluggish." The lack of CSF flow in the subarachnoid space over the convexity of the brain has been repeatedly confirmed in subsequent studies. It was never seriously considered mainly due to the technical difficulty encountered during the observation of CSF flow at this site in live animals. Postmortem analysis was required to determine the CSF drainage pathway in pathological and radioisotope studies [3, 6, 8, 9, 13, 25, 26]. The

physiological CSF dynamics in individual animals, therefore, could not be traced. Unlike techniques used in previous studies, MRI enabled the real time observation of CSF kinetics over the convexity of brain in individual live animals. Although a large portion of the signal intensity change was observed in the nasal mucosa and periorbital region, almost no signal intensity change was observed in the subarachnoid space of the brain convexity, adjacent to the superior sagittal sinus, where the arachnoid villi are located. This finding does not contradict the finding of very-sluggish CSF flow on brain convexity observed by Weed [25]; however, in the guinea pig, it is less likely that a large portion of the CSF flows toward the region of the arachnoid villi. Hydrocephalus is characterized by the abnormal accumulation of CSF in the central nervous system. With the exception of CSF overproduction [27], hydrocephalus in all cases develops due to increased CSF outflow resistance; therefore, CSF dynamics are altered in hydrocephalus [1, 18, 28]. In arrested hydrocephalus, the rate of absorption must be equal to the rate of formation. In progressive hydrocephalus, only a minute fraction of the total amount of secreted CSF is retained. Thus, even in hydrocephalus, the overwhelming majority of CSF formed still egresses somewhere. It has been repeatedly shown, experimentally and clinically, that in hydrocephalus the CSF migrates through the ventricle ependymal wall into the brain parenchyma [16, 29-31]. However, the site of drainage or absorption of the migrated CSF in the hydrocephalic brain remains unresolved. Therefore, it is important to develop an animal model that can investigate the CSF pathway solely from the ventricle, which is separated from the CSF in the subarachnoid space. Based on our observation of the V group, which mimics acute obstructive hydrocephalus in a clinical setting, CSF from the ventricle first migrates into the interstitial space of the brain parenchyma (olfactory lobes) and then subsequently drains into the nasal mucosa. CSF drainage to the periorbital region is not the case in V group that was the noticeable in SAS group. It proposes that the perivascular space that is involved in the interstitial fluid drainage may be a reliable candidate in the brain parenchyma to channel the migrated CSF into the subarachnoid space and then

divert it to the nasal mucosa [6, 32, 33]. Guinea pig has well developed olfactory ventricles that were prolonged from lateral ventricles. Migrated CSF in the olfactory lobe drained through brain parenchyma into subarachnoid space adjacent to the olfactory lobes. The reason of why much CSF did not egress through periorbital region in even high pressure V group is not certain. Nevertheless, one may possible to speculate that the subarachnoid space around the periorbital region collapsed by the enlarged ventricles so that the accumulated CSF in olfactory subarachnoid space may not reach the periorbital region in this group. CSF drainage was increased when CSF pressure rose so that postural changes alter the volume of CSF drainage. However, alteration of the CSF drainage sites by postural changes was uncertain. In this study, animal was placed in prone position that is physiological position for rodent. Investigation of CSF drainage sites alteration by postural changes is interesting and possible to investigate with MRI CSF tracer study. Although this result does not exclude the possibility of CSF absorption by the brain parenchyma through the brain capillaries, a large fraction of the CSF migrating from the ventricle to the brain parenchyma was drained into the nasal mucosa and periorbital region even in the hydrocephalic guinea pig brain.

CONCLUSION

Most of the CSF drainage from the subarachnoid space and the ventricle was observed to be via the nose and periorbital pathway at a rate directly proportional to the CSF pressure. The absence of a parasagittal signal reduces the likelihood of any significant CSF absorption into the superior sagittal sinus via the "classic" pathway. The CSF flow can be monitored under MRI using gadoteridol in a semi-quantitative manner.

REFERENCES

- 1) Davson, H., K. Welch, and M.B. Segal. *Physiology and Pathophysiology of the cerebrospinal fluid*. 1987, New York, Edinburgh: Churchill Livingstone.
- 2) Weed, L.H. Studies on cerebro-spinal fluids. No. III. The pathways of escape from the subarachnoid spaces with particular reference to the arachnoid villi. *J Med Res*, 1921. 31: 51-91.
- 3) Bradbury, M.W., H.F. Cserr, and R.J. Westrop. Drainage of cerebral interstitial fluid into deep cervical lymph of the rabbit. *Am J Physiol*, 1981. 240(4):

- F329-36.
- 4) Cserr, H.F. and P.M. Knopf Cervical lymphatics, the blood-brain barrier and the immunoreactivity of the brain: a new view. *Immunol Today*, 1992. 13(12): 507-12.
 - 5) Boulton, M., *et al.* Raised intracranial pressure increases CSF drainage through arachnoid villi and extracranial lymphatics. *Am J Physiol*, 1998. 275(3 Pt 2): R889-96.
 - 6) Yamada, S., *et al.* Albumin outflow into deep cervical lymph from different regions of rabbit brain. *Am J Physiol*. Vol. 261. 1991. H1197-204.
 - 7) Cserr, H.F., C.J. Harling-Berg, and P.M. Knopf Drainage of brain extracellular fluid into blood and deep cervical lymph and its immunological significance. *Brain Pathol*, 1992. 2(4): 269-76.
 - 8) Erlich, S.S., *et al.* Ultrastructural morphology of the olfactory pathway for cerebrospinal fluid drainage in the rabbit. *J Neurosurg*, 1986. 64(3): 466-73.
 - 9) Szentistvanyi, I., *et al.* Drainage of interstitial fluid from different regions of rat brain. *Am J Physiol*, 1984. 246(6 Pt 2): F835-44.
 - 10) Cserr, H.F., Harling-Berg, C., Ichimura, T., Knopf, P., Yamada, S. Drainage of cerebral extracellular fluids into deep cervical lymph: an afferent limb in brain/immune system interrelations. *Pathophysiology of the blood-brain barrier*, ed. B.B. Johansson, Owman, Ch., Wider, H. Vol. 36. 1990, New York Berlin: Elsevier Science Publishers. 413-420.
 - 11) McComb, J.G., Hyman, S. Lymphatic drainage of cerebrospinal fluids in the primate. *Pathophysiology of the blood-brain barrier*, ed. B.B. Johansson, Owman, Ch., Wider, H. Vol. 38. [Cserr, 1992 #9] 1990: Elsevier Science Publishers. 421-438.
 - 12) McComb, J.G., *et al.* Cerebrospinal fluid drainage as influenced by ventricular pressure in the rabbit. *J Neurosurg*, 1982. 56(6): 790-7.
 - 13) Boulton, M., *et al.* Determination of volumetric cerebrospinal fluid absorption into extracranial lymphatics in sheep. *Am J Physiol*, 1998. 274(1 Pt 2): R88-96.
 - 14) Boulton, M., *et al.* Lymphatic drainage of the CNS: effects of lymphatic diversion/ligation on CSF protein transport to plasma. *Am J Physiol*, 1997. 272(5 Pt 2): R1613-9.
 - 15) Schwalbe G. Der Arachnoidalraum ein Lymphraum und sein Zusammen mit den Perichoroidalraum. *Zentralbl Med Wiss*, 1869. 7: 465-467.
 - 16) Shoesmith, C.L., R. Buist, and M.R. Del Bigio Magnetic resonance imaging study of extracellular fluid tracer movement in brains of immature rats with hydrocephalus. *Neurol Res*, 2000. 22(1): 111-6.
 - 17) James, A.E., Jr., *et al.* The effect of cerebrospinal fluid pressure on the size of drainage pathways. *Neurology*, 1976. 26(7): 659-63.
 - 18) McComb, J.G. Recent research into the nature of cerebrospinal fluid formation and absorption. *J Neurosurg*, 1983. 59(3): 369-83.
 - 19) Del Bigio, M.R. Future directions for therapy of childhood hydrocephalus: a view from the laboratory. *Pediatr Neurosurg*, 2001. 34(4): 172-81.
 - 20) Bui, J.D., *et al.* In vivo dynamics and distribution of intracerebroventricularly administered gadodiamide, visualized by magnetic resonance imaging. *Neuroscience*, 1999. 90(3): 1115-22.
 - 21) Del Bigio, M.R., C.R. Crook, and R. Buist Magnetic resonance imaging and behavioral analysis of immature rats with kaolin-induced hydrocephalus: pre- and postshunting observations. *Exp Neurol*, 1997. 148(1): 256-64.
 - 22) Rocklage, S.M. and A.D. Watson Chelates of gadolinium and dysprosium as contrast agents for MR imaging. *J Magn Reson Imaging*, 1993. 3(1): 167-78.
 - 23) Erlich, S.S., *et al.* Ultrastructure of the orbital pathway for cerebrospinal fluid drainage in rabbits. *J Neurosurg*, 1989. 70(6): 926-31.
 - 24) McComb, J.G., Hyman, S. Lymphatic drainage of cerebrospinal fluids in the primate. *Pathophysiology of the blood-brain barrier*, ed. B.B. Johansson, Owman, Ch., Wider, H. Vol. 38. 1990: Elsevier Science Publishers. 421-438.
 - 25) Weed, L.H. Studies on cerebrospinal fluids. No. III. The pathways of escape from the subarachnoid spaces with particular reference to the arachnoid villi. *J Med Res*, 1914. 31: 51-91.
 - 26) Weed, L.H., Hughson W Intracranial venous pressure and cerebrospinal fluid pressure as affected by the intravenous injection of solutions of various concentration. *Am J Physiol*, 1921(58): 101-130.
 - 27) Eisenberg, H.M., J.G. McComb, and A.V. Lorenzo Cerebrospinal fluid overproduction and hydrocephalus associated with choroid plexus papilloma. *J Neurosurg*, 1974. 40(3): 381-5.
 - 28) Massicotte, E.M., R. Buist, and M.R. Del Bigio Altered diffusion and perfusion in hydrocephalic rat brain: a magnetic resonance imaging analysis. *J Neurosurg*, 2000. 92(3): 442-7.
 - 29) Mori, K., *et al.* [Pathogenesis of periventricular lucency on computed tomography (author's transl)]. *Neurol Med Chir (Tokyo)*, 1980. 20(9): 947-55.
 - 30) Moseley, I.F. and E.W. Radu Factors influencing the development of periventricular lucencies in patients with raised intracranial pressure. *Neuroradiology*, 1979. 17(2): 65-9.
 - 31) Murata, T., *et al.* The significance of periventricular lucency on computed tomography: experimental study with canine hydrocephalus. *Neuroradiology*, 1981. 20(5): 221-7.
 - 32) Cserr, H.F. Role of secretion and bulk flow of brain interstitial fluid in brain volume regulation. *Ann N Y Acad Sci*, 1988. 529: 9-20.
 - 33) Ichimura, T., P.A. Fraser, and H.F. Cserr Distribution of extracellular tracers in perivascular spaces of the rat brain. *Brain Res*, 1991. 545(1-2): 103-13.